

## MICROINDUCTORS FOR SPACECRAFT POWER ELECTRONICS

Erik Brandon, Emily Wesseling, Victor White, Udo Lieneweg,  
Hilary Cherry and Judith Podosek  
*Center for Integrated Space Microsystems*  
*Jet Propulsion Laboratory*  
*California Institute of Technology*  
*4800 Oak Grove Drive*  
*Pasadena, CA 91109*

Amri Hernandez-Pellerano  
*NASA Goddard Spaceflight Center*  
*8800 Greenbelt Road*  
*Greenbelt, MD 20771*

### ABSTRACT

Several investigations over the last 20 years in the area of thin and thick film magnetic microinductors have yielded promising results. Future work, however, will need to focus on the design of these components for specific applications. Application to a dc-dc converter will require optimization of the inductor for power density and efficiency at a given frequency, primarily through choice of appropriate materials and optimal component design. Classical magnetic and electric circuit analysis as well as finite element analysis may be applied to optimize the design for maximum inductance per unit area and maximum power density. Moving to higher frequencies enables smaller inductance values, but will result in increased core losses due to eddy currents, ferromagnetic resonance or domain wall motion. This paper will focus on the development of microinductors for a 1-10 MHz integrated dc-dc converter for space applications.

### INTRODUCTION

The next generation of smaller planetary spacecraft will require reductions in the mass and volume of the power electronics (1). A significant barrier to miniaturization of the power subsystems are the dc-dc converters, which rely on discrete magnetic components such as inductors and transformers. Inductors are an integral component in converters, serving as both energy storage and filtering elements. As converters move toward higher operating frequencies and as output voltages migrate to lower levels, smaller inductive elements can be used.

Planar inductors can be fabricated on various substrates and even on silicon die next to active devices by using a metal spiral trace, patterned from one or more of the metallization layers of a standard complementary metal oxide semiconductor (CMOS) process (2). These "air core" inductors are typically used for microwave applications at frequencies of 1 GHz or higher, where sufficient Q factors are attainable. These simple

air core inductors are unsuitable for power converters, however, which usually operate in the 250 kHz to 1 MHz range.

Higher value “microinductors” that are useable at lower frequencies may be constructed using standard microelectronic fabrication techniques through the addition of magnetic films deposited above and below the spiral plane (3-11). The magnetic layers serve as “cores” to enclose the flux generated by the spiral, and can in theory enhance the inductance by a factor of  $\mu_r$ , the relative permeability of the magnetic material. Since ferrite materials (which are used in conventional power magnetics) require high temperature processing, ferromagnetic films that may be grown by conventional vacuum deposition techniques or electroplating are typically used.

Furthermore, copper metallization layers (versus the aluminum metallization used in standard CMOS processes) can be employed to reduce the series resistance of the inductor and limit subsequent  $I^2R$  power losses. Low temperature processes afford the possibility of monolithic converters, in which the inductor is added to an active silicon die in a post-processing step. Alternatively, advanced packaging techniques may also be used to interconnect the inductor to the rest of the converter.

Although microinductors displaying relatively high inductance values can be fabricated using such an approach, implementing these components in power applications requires overcoming several significant design challenges. Despite the fact that several models exist for the design of air core inductors (12), similar models must be developed to enable accurate prediction of microinductor behavior and facilitate subsequent design of these components (13). Also, processes must be developed to implement such designs, and account for design parameters such as “gaps,” which are often used in discrete inductors to extend the range of currents over which the inductor is operable. Finally, the use of metallic magnetic materials present several challenges, including the introduction of parasitic capacitances which lower the self-resonant frequency of the inductor and eddy current losses which may be significant at the required frequencies of 1-10 MHz.

## EXPERIMENTAL

The microinductors were fabricated using electroplating in conjunction with thick photoresist techniques. A standard inductor cross-section is depicted schematically in Figure 1. Glass substrates were used to eliminate parasitic capacitances and limit losses within the substrate. A standard Permalloy bath was used containing 39.0 g/L of nickel (II) chloride hexahydrate, 16.3 g/L of nickel (II) sulfate hexahydrate, 25.0 g/L of boric acid, 1.5 g/L of sodium saccharin dihydrate, 25.0 g/L of sodium chloride, 0.05 g/L of sodium dodecyl sulfate and 1.4 g/L of iron (II) sulfate heptahydrate. A nickel anode was used, and the bath pH was adjusted to about 2.80 with hydrochloric acid. The electroplating was carried out at a current density of 5 mA cm<sup>-2</sup> using an EG&G Instruments/Princeton Applied Research Model 273A Potentiostat/Galvanostat.

The lower magnetic layer was defined with an AZ 5000 series photoresist on an underlying evaporated seed layer of 500 Å of Au (with a 100 Å evaporated Cr film between the Au film and glass substrate as an adhesion layer). The Ni-Fe film was plated using the standard Permalloy bath. After stripping the photoresist with acetone and etching and removal of the electroplating seed layer using Ar ion milling, the magnetic

layer was coated with AZ 5214 photoresist as a lower insulating layer, which was patterned with a UV exposure and subsequent development. Next, copper coils were electroplated (using a commercial acid copper bath) on top of this insulating layer, again using a Cr/Au seed layer and an AZ 5000 series photoresist to define the coils. The coils were then planarized using a multi-step application of SU-8 photoresist involving multiple applications of the resist, followed by subsequent UV exposure, post-exposure bake and development. The number of applications varied, with thicker coils requiring multiple spin coatings. The top magnetic layer was then deposited in a similar manner to the bottom magnetic layer. Finally, the photoresist was stripped using acetone, and the seed layer etched using Ar ion milling. A finished array of microinductors is depicted in Figure 2.

All electrical measurements were made on an HP 4284A impedance analyzer and an HP 8753B network analyzer with appropriate probe tips. Magnetic measurements were made on thin films deposited on Cr/Pt/Au coated oxidized silicon wafers using a vibrating sample magnetometer.

## DISCUSSION

Various approaches to the fabrication of microinductors have been demonstrated over the last 20 years. One approach involves the sputter deposition of magnetic films for use as the core material, which has been successfully employed to achieve moderate enhancements of the air core value (3-8). Sputtering is an attractive method which can be used to deposit a wide range of magnetic materials, including alloys and oxides with resistivities  $>100 \mu\Omega\text{-cm}$  which are useful in limiting eddy current losses. For example Co-Zr based films (4-8) and Co-Fe-Hf-O films (14) have been deposited and show promising characteristics at frequencies higher than 1 MHz. Problems arise, however, when films  $>1 \mu\text{m}$  thick are employed as the core.

Not only is sputtering a more costly method than electroplating, but inherent problems arise from the etching of thick ( $>1 \mu\text{m}$ ) metallic films. Whereas electroplating is an additive process (amenable to the deposition of thick films ideal for microinductor cores with large cross-sectional areas) sputtering films requires a subtractive process involving either wet or dry etching. Dry etching of thick films usually involves long etch times resulting in heating of the substrate (and potential degradation of the magnetic film properties), while wet etching of thick films typically results in severe undercutting and subsequent delamination of the layers.

We investigated such an approach using thick rf sputtered Co-Zr alloys. Although it is possible to construct such structures with a magnetic film thickness of  $1 \mu\text{m}$  or less, etching thicker layers usually resulted in removal of the entire film due to severe undercutting. Lift-off methods (in which the magnetic films are sputtered into a photoresist pattern and the photoresist removed to define the pattern) are difficult to implement due to the long sputtering times, during which the plasma tends to degrade and bake the photoresist.

This restriction in cross-sectional area limits the overall specific inductance, requiring an electroplated process (9-11). To remain competitive with surface mount technologies, large specific inductances of  $\geq 1 \mu\text{H mm}^{-2}$  should be achieved (at 1 MHz),

with subsequent resistances on the order of  $1 \Omega$  or less to maintain sufficient converter efficiency. In designing our microinductors, several factors were initially considered.

First, the Greenhouse method (12) was used to determine the air core value of a variety of coil geometries. Next, a library of inductors featuring a range of line widths, line spacings, areas, number of turns and magnetic film thicknesses were fabricated, to empirically determine the maximum enhancement in inductance over the air core value that is attainable at 1 MHz with the existing process. Finally, factoring in the maximum enhancement, new inductors were then designed to achieve the targeted specific inductance with minimal resistance.

A schematic of the fabricated microinductors is shown in Figure 1, with an actual top view SEM micrograph of an array of microinductors shown in Figure 2. The design features an electroplated coil with magnetic layers above and below the plane of the spiral. Insulating photoresist dielectric layers are deposited between the magnetic and conducting layers to prevent shorting. Although the magnetic and electrical properties of Permalloy are not ideal for inductor applications, this material was used due to its ease of deposition and the well defined properties. A typical magnetization curve for the Permalloy used in these inductors is shown in Figure 3.

Minimizing the series resistance of the inductor is also key in designing an adequate inductor. A figure of merit for magnetic devices “Q” can be defined as the energy stored by the inductor (proportional to the inductance) divided by the energy dissipated (proportional to the resistance). As series resistance increases, power dissipation and the potential for self-heating phenomena similarly increase. For microinductors, thick electroplated metallization layers can be readily utilized to reduce these power losses (as opposed to the thinner aluminum layers used for on-chip inductors which are limited by fabrication design rules). Ultimately, these power losses result in diminished, load-dependent converter output voltages and reduced converter efficiencies. A typical electroplated coil that we deposited is depicted in Figure 4.

Inductance and resistance data vs. frequency of the coil current for one of the inductors from our initial library of components is shown in Figure 5. This microinductor is comprised of  $15 \mu\text{m}$  thick, 10-turn copper coils with dimensions of  $0.6 \text{ mm} \times 1 \text{ mm}$ . Several “slits” running perpendicular to the length of the coils were patterned into the magnetic layers, to reduce eddy current losses within the core. The top magnetic layer, comprised of  $10 \mu\text{m}$  of Permalloy, is visible from the SEM micrograph in Figure 2, along with the copper bond pads used for measurement. As seen in Figure 4, a high specific inductance of about  $1 \mu\text{H mm}^{-2}$  is obtained at 1 MHz, with a coil resistance of less than  $3 \Omega$ . The inductance drops off rapidly as a function of frequency, with the coil resistance increasing due to skin depth effects.

For this particular inductor, an order of magnitude enhancement in inductance over the air core inductance is observed (based on the predicted air core specific inductance of  $110 \text{ nH mm}^{-2}$ ). This represents a significant enhancement in the air core inductance at 1 MHz. It also represents a significant specific inductance, particularly for an inductor with only 10 turns. Typically, such high inductance values require many more turns to achieve a comparable value. A key trade-off involves further patterning the magnetic layers to reduce eddy currents, while maintaining sufficient core volume to raise the

inductance. Furthermore, these eddy current patterns will not only reduce the overall volume of the core, but alter the domain structure and magnetization of the material which may significantly influence inductor performance.

By increasing the frequency of operation, even smaller values of inductance can be tolerated for the converter applications, but will most likely require different, higher resistivity materials. Another design concern for the inductors is the influence of a dc bias current on the overall inductance (8). A dc current equal to the load current will flow through the inductor when made part of a dc-dc converter, which may degrade the inductance by saturating the core.

The normalized inductance as a function of applied dc current for the 0.6 mm<sup>2</sup> inductor described above is displayed in Figure 6. As seen from the data, at 100 mA the inductance has dropped to less than 50% the zero bias value. It is possible that this effect may be minimized by controlling the gap at the edge of the inductor, where the top and bottom magnetic layers meet. We are currently investigating this effect. Also, soft magnetic materials with high anisotropy fields and large saturation magnetizations can be utilized, to prevent saturation while maintaining sufficient core permeability.

Although, higher inductances can be obtained by simply adding more turns, thicker copper layers or wider coil turns must be used to offset the increase in resistance. Future designs will feature coils which minimize negative mutual coupling in the center of the coil, combined with optimal patterning of the layers. Approaches used for analyzing read-write heads may be adapted for inductor modeling (13). We are currently using 3-D magnetic simulations to better understand these phenomena. These test structures will also be packaged and characterized in board level dc-dc converters.

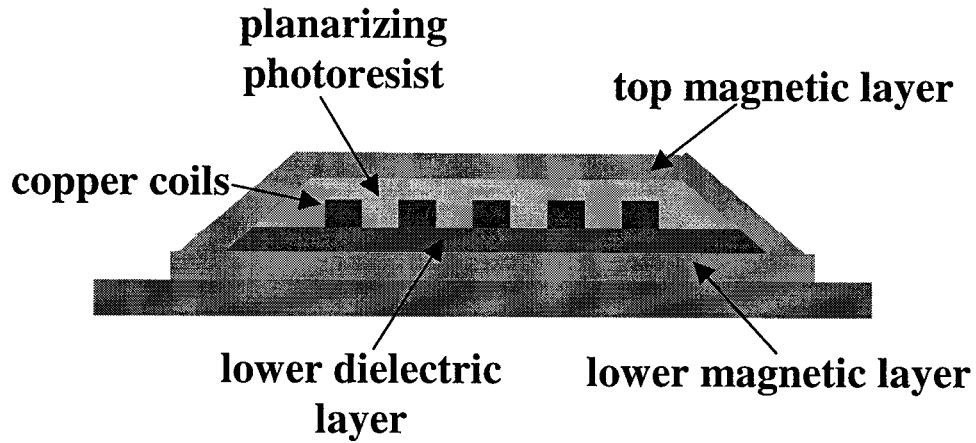
#### ACKNOWLEDGEMENTS

The authors wish to acknowledge the NASA Deep Space Systems Technology Program and the JPL Center for Integrated Space Microsystems for their financial support, as well as Elizabeth Kolawa of JPL and Professor Marc Nicolet at the California Institute of Technology for their advice and assistance. The research described in this paper was carried out at the Jet Propulsion Laboratory, California Institute of Technology, under a contract with the National Aeronautics and Space Administration.

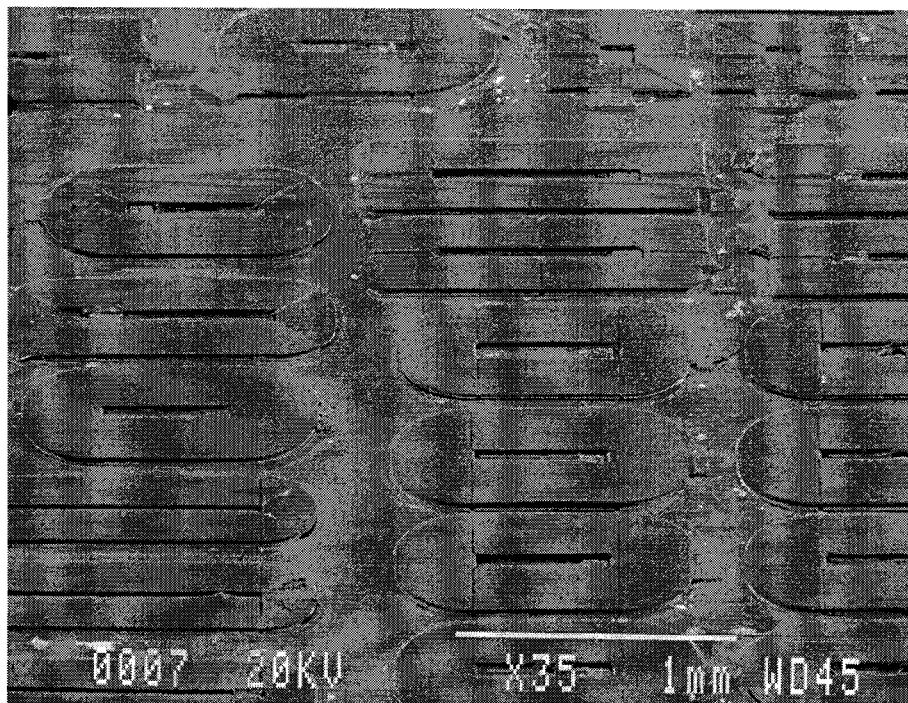
#### REFERENCES

1. R. Detwiler, S. Surampudi, P. Stella, K. Clark and P. Bankston, *J. Prop. Power*, **12**, 828 (1996).
2. R.A. Pucel, *IEEE Trans. Microwave Theory Tech.*, **MTT-29**, 513 (1981).
3. R.F. Soohoo, *IEEE Trans. Magn.* **15**, 1803 (1979).
4. K. Kawabe, H. Koyama and K. Shirai, *IEEE Trans. Magn.*, **MAG-20**, 1804 (1984).
5. M. Yamaguchi, S. Arakawa, H. Ohzeki, Y. Hayashi and K.I. Arai, *IEEE Trans. Magn.*, **28**, 3015 (1992).
6. V. Korenivski and R.B. van Dover, *J. Appl. Phys.*, **82**, 5247 (1997).
7. T. Sato, H. Tomita, A. Sawabe, T. Inoue, T. Mizoguchi and M. Sahashi, *IEEE Trans. Magn.* **30**, 217 (1994).

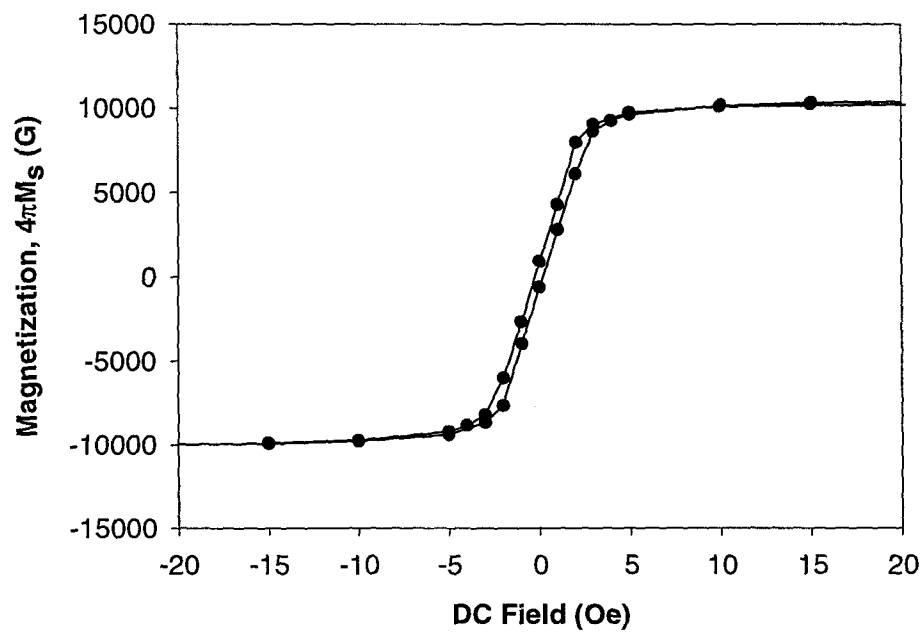
8. M. Yamaguchi, H. Okuyama and K.I. Arai, *IEEE Trans. Magn.* **31**, 4229 (1995).
9. C.H. Ahn and M.G. Allen, *IEEE Trans. Magn.* **30**, 73 (1994).
10. C.H. Ahn and M.G. Allen, *IEEE Trans. Magn.* **11**, 239 (1996).
11. T.M. Liakopoulos and C.H. Ahn, *IEEE Trans. Magn.*, **35**, 3679 (1999).
12. H.M. Greenhouse, *IEEE Trans. Parts, Hybrids, Packaging*, **PHP-10**, 101 (1974).
13. R.E. Jones, Jr., *IEEE Trans. Magn.* **MAG-14**, 509 (1978).
14. A. Makino and Y. Hayakawa, *Mater. Sci, Eng.*, **A181/A182**, 1020 (1994).



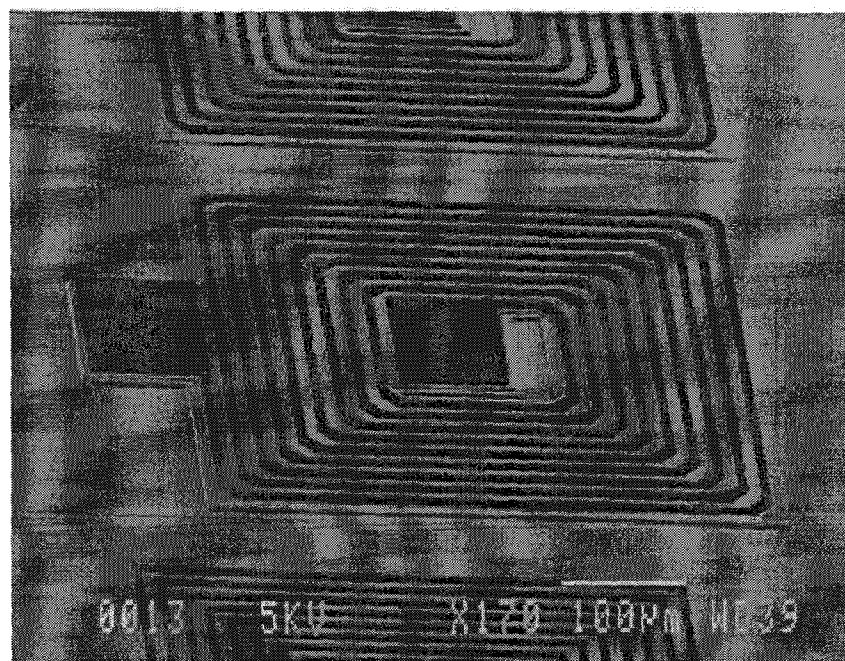
**Figure 1.** Schematic cross-section of a microfabricated inductor. The degree of slope at the edges of the device, as well as the amount of overlap between the top and bottom magnetic layers are largely a function of the specific processing conditions used for the planarizing photoresist.



**Figure 2.** Top view of an array of electroplated microinductors on a glass substrate.



**Figure 3.** Magnetization vs. applied field for electroplated Permalloy used in the reported microinductors.



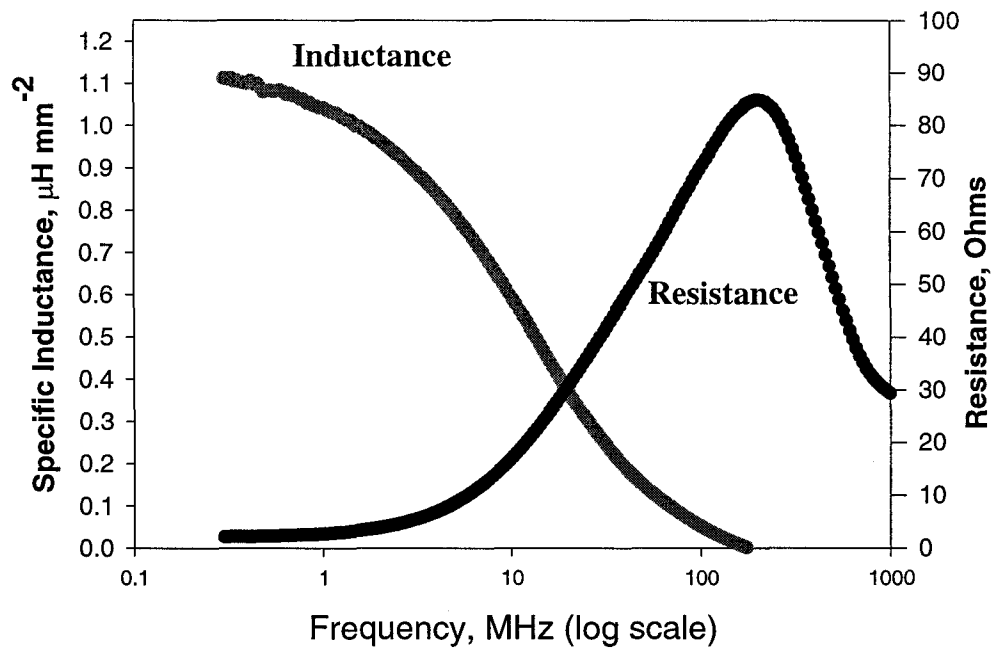


**Figure 4.** SEM micrograph of a typical electroplated coil, prior to planarization with the SU-8 photoresist and deposition of the top magnetic layer.

**Figure 5.** Specific inductance vs. frequency for the  $0.6 \text{ mm}^2$  microinductor described in the text.

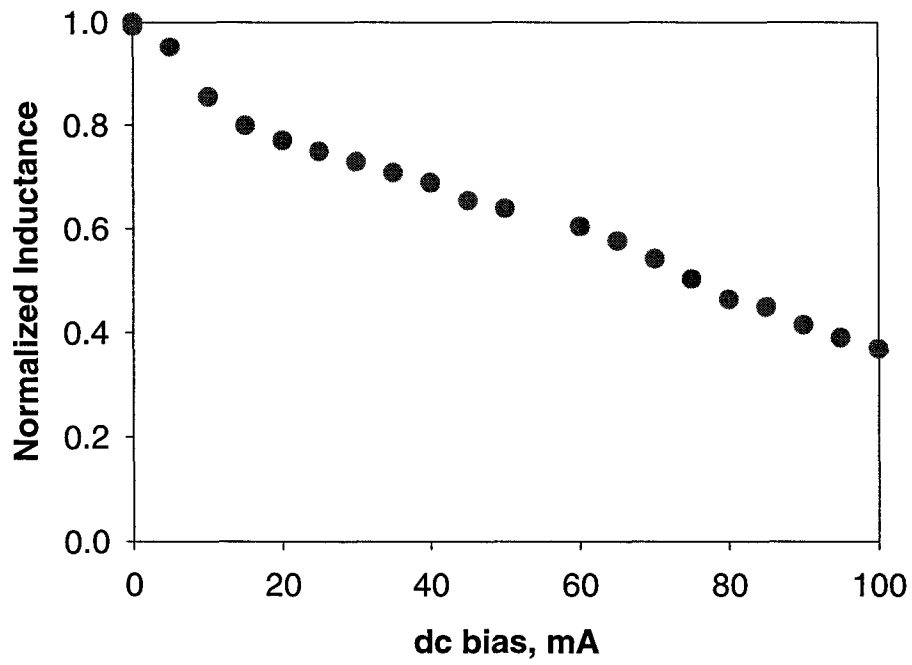


**Figure 6.** Normalized inductance vs. applied dc bias current for the 0.6 mm<sup>2</sup> microinductor (at 10 mA rms excitation current).